ELSEVIER

Composite Structures 48 (2000) 245–260

COMPOSITE STRUCTURES

A priori vs. a posteriori evaluation of transverse stresses in multilayered orthotropic plates

Erasmo Carrera

DIAS, Politecnico di Torino, Corso Duca degli Abruzzi 24, 10129 Torino, Italy

Abstract

A comprehensive analysis of available models and techniques to evaluate transverse shear and normal stresses in multilayered orthotropic plates is given in this paper. Transverse stresses evaluated a posteriori by integration of the 3D indefinite equilibrium equations and from Hooke's law are compared to those given a priori by an assumed stress model (if implemented). Classical theories formulated on the basis of assumed through-the-thickness displacement fields as well as mixed modelings originated by a Reissner's mixed variational theorem are considered. Both cases of Equivalent Single Layer Models (ESLMs) and Layer Wise Models (LWMs) have been investigated. Linear up to fourth N-order expansions, in the thickness layer/plate direction, have been implemented for the introduced displacement and stress fields. As a result, theories describing so-called zigzag effects and accounting for interlaminar continuous transverse stresses are compared to simplified cases which neglect zigzag and violate interlaminar equilibrium. A numerical investigation has been restricted to bending of simply supported, orthotropic plates. It is mainly concluded that: (1) N-order increasing, layer-wise analysis could furnish excellent a priori as well as a posteriori description of transverse stresses of laminate thick and thin plates; ESLM accuracy remains subordinate to laminate lay-out, to plate thickness and to two-dimensional modelings (mixed results are much more accurate than classical ones). (2) The discrepancy among the three manners of evaluating transverse shear stresses is scarcely dependent on plate thickness ratio. (3) In most of the considered cases, the best description of transverse stresses has been obtained by layer-wise mixed analysis upon integration of the 3D indefinite equilibrium equations.

Keywords: Transverse stresses; Multilayered orthotropic plates

1. Introduction

The manner in which in-plane $\{\boldsymbol{\sigma}_p\}$ and transverse stresses $\{\boldsymbol{\sigma}_n\}$ are determinate in the analysis of structures is subordinate to the theory adopted to model the 3D-continuum. Firstly, this manner rests on the employed formulation [1]. Classical formulations based on displacement assumptions lead to a posteriori calculation of stresses via Hooke's law written in terms of stiffness coefficients, e.g. Eq. (1). Stresses are a priori evaluated for those formulations based on stress assumptions. Mixed formulations lead to mixed cases: assumed stresses are evaluated a priori while the others are derived by the assumed stress and displacement variables (via Hooke's law written in mixed form, e.g. Eq. (2). Secondly, in case of one- or two-dimensional modeling structures (e.g. beams, plates or shells) stress evaluation depends on the approximated theory that had been used to solve the 3D continuum. In particular, the calculation of transverse stress components $\{\boldsymbol{\sigma}_n\}$ is very much subordinate to the adopted approximations. For instance, Kirchhoff's plate theory which neglects transverse shear and normal deformations, permits a posteriori evaluations of in-plane stresses $\{\boldsymbol{\sigma}_p\}$ while transverse stresses cannot be calculated a posteriori by any Hooke's law. On the other hand, it is well known that for this plate theory (see for example [2]) there exists a further technique to compute transverse shear components of $\{\boldsymbol{\sigma}_n\}$ a posteriori. Such a technique employs the indefinite equilibrium equations of 3D elasticity: in-plane stresses are integrated in the thickness directions, e.g. Eq. (5). There are other cases, for instance Reissner–Mindlin shear deformable plate theory, in which a posteriori evaluation of transverse shear stresses via Hooke's law even though possible is not convenient. Hooke's law in this case would lead to constant transverse shear stresses then violating homogeneous conditions in correspondence to the top/bottom plate surfaces. The use of the indefinite equilibrium equations is therefore preferred. It is concluded that: (i) transverse stresses can be calculated in three manners (one a priori, the other two are given a posteriori); (ii) the accuracy of these three

0263-8223/00/$ - see front matter
PII: S0263-8223(99)00112-9

manners is very much subordinate to the approximations introduced by the employed two-dimensional theories.

Layered structures deserve special attention. These are characterized by a non-continuous thermo-mechanical material property distribution in the thickness direction. In addition, most of the layered structures employed in aerospace, automotive and ship industry are made of composite materials. These materials exhibit higher values of Young's moduli orthotropic ratio ($E_L/E_T = E_L/E_z = 5:40$, L denotes the fiber directions while T and z are two-direction orthogonal to L) and the lower transverse shear moduli ratio ($G_{LT}/E_L \approx G_{TT}/E_L = 1/10:1/200$) leading to higher transverse shear and normal stress deformability in comparison to isotropic cases. As a consequence, accurate modelings of such structures (see exact analyses in [3–6]) require the description of interlaminar continuous transverse stresses (both shear and normal components). In order to improve the transverse stress fields of classical plate theories (such as those based on Kirchhoff or Reissner–Mindlin assumptions) a number of refined theories have been proposed in the last three decades. Among these refined theories a convenient distinction can be made between models in which the number of unknown variables is independent or dependent by the number of constitutive layers of the plates. Following Reddy [2], to the first grouping we assign the name Equivalent Single Layer Models (ESLM) while Layer Wise Model (LWM) is used to denote the others. Many ESLMs have been proposed which furnish interlaminar continuous transverse shear stresses [7–19]. Interlaminar continuous transverse normal stresses were accounted for in the mixed model by Toledano and Murakami [13]. However, the accuracy of ESLMs is problem dependent. Early LWMs [20,21] and recent [22–30] LWMs have shown the superiority of layer-wise approaches with respect to ESL ones to accurately predict transverse stress response response of thick and very thick structures. The best results have been obtained by mixed LWMs [28,30] which a priori describe interlaminar continuous transverse normal stress. More exhaustive overviews on classical and refined models of multilayered structures have been reported in many published review articles. Among these one mentions the papers [31–34] and the recent book by Reddy [2].

To the best of the author's knowledge a comprehensive study is not available in which the three manners to compute transverse stresses are compared for both cases of mixed and classical formulation as well as for ESLM and LWM analysis. Based on this fact, this paper has the aim to contribute, with the help of numerical illustration, to a better understanding of the conditions under which the three mentioned methods to compute transverse stresses can be used in a reliable sense. In other words, this paper would investigate the influence of the order of the expansion used in the introduced displacement and/or stress fields, of laminate lay-outs, of geometrical parameters and of mechanical properties of the lamina on the foregoing mentioned classical and refined two-dimensional plate theories. To this purpose, both LW amd ESL mixed models based on Reissner's mixed variational theorem [35,36] as well as classical formulations based on principle of virtual displacements have been considered. Existing mixed [13,22,26–28] and classical [10,21,23] have been extended to describe up to the fourth-order transverse stresses and/or displacements fields in the thickness plate/layer direction. All these theories have been formulated in a unified form. Related governing equations have been conveniently written in array form by referring to techniques developed by the author in previous works [26–30,38,39]. Closed form solutions have been restricted to plates made by orthotropic layers.

2. Preliminary

The geometry and coordinate systems of the multilayered plate of N_l layers are shown in Fig. 1 The integer k, which is extensively used as both subscripts or superscripts, denotes the layer number that starts from the plate-bottom. x and y are the plate middle surface Ω^k coordinates. Γ^k is the layer boundary on Ω^k. z and z_k are the plate and layer thickness coordinates; h and h_k denote the plate and layer thicknesses, respectively. $\zeta_k = 2z_k/h_k$ is the non-dimensioned local plate-coordinate; A_k denotes the k-layer thickness domain. Symbols that are not affected by the k subscript/superscripts refer to the whole plate.

2.1. Hooke's law

The lamina are considered to be homogeneous and operate in the linear elastic range. Stiffness coefficients

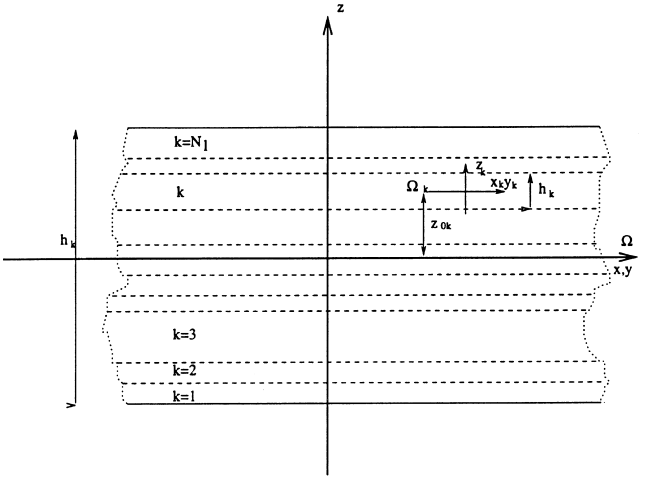

Fig. 1. Multilayered plate.

are employed in standard form of Hooke's law for the anisotropic k-lamina. This reads $\sigma_i = \tilde{C}_{ij}\epsilon_j$, where the sub-indices i and j, ranging from 1 to 6, stand for the index couples 11, 22, 33, 13, 23 and 12, respectively. The material is assumed to be orthotropic as specified by $\tilde{C}_{14} = \tilde{C}_{24} = \tilde{C}_{34} = \tilde{C}_{64} = \tilde{C}_{15} = \tilde{C}_{25} = \tilde{C}_{35} = \tilde{C}_{65} = 0$. This implies that σ^k_{xz} and σ^k_{yz} depend only on ϵ^k_{xz} and ϵ^k_{yz}. In matrix form,

$$\begin{aligned} \boldsymbol{\sigma}^k_{p\mathrm{H}_d} &= \tilde{\boldsymbol{C}}^k_{pp}\boldsymbol{\epsilon}^k_{p\mathrm{G}} + \tilde{\boldsymbol{C}}^k_{pn}\boldsymbol{\epsilon}^k_{n\mathrm{G}}, \\ \boldsymbol{\sigma}^k_{n\mathrm{H}} &= \tilde{\boldsymbol{C}}^k_{np}\boldsymbol{\epsilon}^k_{p\mathrm{G}} + \tilde{\boldsymbol{C}}^k_{nn}\boldsymbol{\epsilon}^k_{n\mathrm{G}}, \end{aligned} \tag{1}$$

where

$$\tilde{\boldsymbol{C}}^k_{pp} = \begin{bmatrix} \tilde{C}^k_{11} & \tilde{C}^k_{12} & \tilde{C}^k_{16} \\ \tilde{C}^k_{12} & \tilde{C}^k_{22} & \tilde{C}^k_{26} \\ \tilde{C}^k_{16} & \tilde{C}^k_{26} & \tilde{C}^k_{66} \end{bmatrix},$$

$$\tilde{\boldsymbol{C}}^k_{pn} = \tilde{\boldsymbol{C}}^{k\mathrm{T}}_{np} = \begin{bmatrix} 0 & 0 & \tilde{C}^k_{13} \\ 0 & 0 & \tilde{C}^k_{23} \\ 0 & 0 & \tilde{C}^k_{36} \end{bmatrix},$$

$$\tilde{\boldsymbol{C}}^k_{nn} = \begin{bmatrix} \tilde{C}^k_{44} & \tilde{C}^k_{45} & 0 \\ \tilde{C}^k_{45} & \tilde{C}^k_{55} & 0 \\ 0 & 0 & \tilde{C}^k_{66} \end{bmatrix}.$$

Bold letters denote arrays. The superscript T signifies array transposition. The subscripts n and p denote transverse (out-of-plane, normal) and in-plane values, respectively. Therefore

$$\boldsymbol{\sigma}^k_p = \left\{\sigma^k_{xx}, \sigma^k_{yy}, \sigma^k_{xy}\right\}, \qquad \boldsymbol{\sigma}^k_n = \left\{\sigma^k_{xz}, \sigma^k_{yz}, \sigma^k_{zz}\right\},$$
$$\boldsymbol{\epsilon}^k_p = \left\{\epsilon^k_{xx}, \epsilon^k_{yy}, \epsilon^k_{xy}\right\}, \qquad \boldsymbol{\epsilon}^k_n = \left\{\epsilon^k_{xz}, \epsilon^k_{yz}, \epsilon^k_{zz}\right\}.$$

Subscript H denotes stresses evaluated with classical form of Hooke's law while subscript G denotes the strain from the geometrical relation Eq. (3). Further, subscript d signifies values employed in the displacement formulation. Eq. (1) is used in conjunction with a standard displacement formulation, while, for the adopted mixed solution procedure, the stress–strain relationships are conveniently put in the following mixed form:

$$\begin{aligned} \boldsymbol{\sigma}^k_{p\mathrm{H}} &= \boldsymbol{C}^k_{pp}\boldsymbol{\epsilon}^k_{p\mathrm{G}} + \boldsymbol{C}^k_{pn}\boldsymbol{\sigma}^k_{nM}, \\ \boldsymbol{\epsilon}^k_{n\mathrm{H}} &= \boldsymbol{C}^k_{np}\boldsymbol{\epsilon}^k_{p\mathrm{G}} + \boldsymbol{C}^k_{nn}\boldsymbol{\sigma}^k_{nM}, \end{aligned} \tag{2}$$

where both stiffness and compliance coefficients are employed. The subscript M states that the transverse stresses are those of the assumed model in Eq. (16) (see the next sections). The relation between the arrays of coefficients in the two forms of Hooke's law is simply found

$$\boldsymbol{C}^k_{pp} = \tilde{\boldsymbol{C}}^k_{pp} - \tilde{\boldsymbol{C}}^k_{pn}\tilde{\boldsymbol{C}}^{k^{-1}}_{nn}\tilde{\boldsymbol{C}}^k_{np}, \quad \boldsymbol{C}^k_{pn} = \tilde{\boldsymbol{C}}^k_{pn}\tilde{\boldsymbol{C}}^{k^{-1}}_{nn},$$
$$\boldsymbol{C}^k_{np} = -\tilde{\boldsymbol{C}}^{k^{-1}}_{nn}\tilde{\boldsymbol{C}}^k_{np}, \quad \boldsymbol{C}^k_{nn} = \tilde{\boldsymbol{C}}^{k^{-1}}_{nn}.$$

Superscript -1 denotes an inversion of the array.

2.2. Strain–displacement relations

The strain components $\boldsymbol{\epsilon}^k_p, \boldsymbol{\epsilon}^k_n$ are linearly related to the displacements $\boldsymbol{u}^k$ ($\{u^k_x, u^k_y, u^k_z\}$), according to the following geometrical relations:

$$\boldsymbol{\epsilon}^k_{p\mathrm{G}} = \boldsymbol{D}_p\boldsymbol{u}^k, \quad \boldsymbol{\epsilon}^k_{n\mathrm{G}} = \boldsymbol{D}_n\boldsymbol{u}^k. \tag{3}$$

$\boldsymbol{D}_p$ and $\boldsymbol{D}_n$ denote in-plane and out-of-plane differential operators

$$\boldsymbol{D}_p = \begin{bmatrix} \partial_x & 0 & 0 \\ 0 & \partial_y & 0 \\ \partial_y & \partial_x & 0 \end{bmatrix}, \quad \boldsymbol{D}_n = \begin{bmatrix} \partial_z & 0 & \partial_x \\ 0 & \partial_z & \partial_y \\ 0 & 0 & \partial_z \end{bmatrix}.$$

2.3. 3D indefinite equilibrium equations

In the static case and in the absence of volume forces the indefinite equilibrium equations of 3D elasticity are

$$\sigma_{ij_{,j}} = 0, \quad i,j = x,y,z, \tag{4}$$

where comma denotes differentiation. In the frame of a two-dimensional modeling, the in-plane stresses and the transverse shear stresses (if available) can be integrated in the thickness z-direction. For instance, if one starts from the layer bottom, transverse shear and normal stresses in the k-layers are

$$\sigma^k_{iz}(z) = \sigma^k_{iz_b} - \int_{z_k}^{z} (\sigma_{iy_{,y}} + \sigma_{ix_{,x}})\,\mathrm{d}z, \quad i = x,y,z, \tag{5}$$

where $\sigma^k_{iz_b}$ is the stress value at the k-layer bottom. The case $i = z$ can be implemented if and only if transverse shear stresses are included in the theories under consideration.

3. Implemented theories

The assumed models in this section illustrated refer to the same order of expansion of the three components for both displacements and transverse stresses. In order to encounter well-known results from the literature, see for example in [10,31,37] or in the author's discussion reported in [26], different polynomial orders should be used in such expansion for the different displacement or transverse stress components. For the sake of brevity, the results related to these aspects have not been discussed in the numerical parts as they do not change the obtained conclusions.

3.1. Classical equivalent single layer models

Firstly, classical models are considered. As usual, the displacement variables are expressed in Taylor series in terms of unknown variables which are defined on the plate reference surface Ω,

$$\boldsymbol{u} = \boldsymbol{u}_0 + z^r \boldsymbol{u}_r, \quad r = 1, 2, \ldots, N. \tag{6}$$

N is a free parameter of the model. Different values for different modelings and different displacement and stress components are assumed. The repeated r indexes are summed over their ranges. Subscript 0 denotes displacement values with correspondence to the plate reference surface Ω. Linear and higher order distributions in the z-direction are introduced by the r-polynomials. The assumed models can be written with the same notations that will be adopted for the layer-wise stress model Eq. (11). Eq. (6) is therefore rewritten as

$$\begin{aligned} &\boldsymbol{u} = F_t \boldsymbol{u}_t + F_b \boldsymbol{u}_b + F_r \boldsymbol{u}_r = F_\tau \boldsymbol{u}_\tau, \quad \tau = t, b, r, \\ &\quad r = 1, 2, \ldots, N-1. \end{aligned} \tag{7}$$

Subscript b denotes values related to the plate reference surface Ω ($\boldsymbol{u}_b = \boldsymbol{u}_0$) while subscript t refers to the highest term ($\boldsymbol{u}_t = \boldsymbol{u}_N$). The F_τ functions assume the following explicit form:

$$F_b = 1, \quad F_t = z^N, \quad F_r = z^r, \quad r = 1, 2, \ldots, N-1. \tag{8}$$

Classical models violate interlaminar equilibria of the transverse stresses. Further they do not describe zigzag form of the displacement field in plate thickness direction.

3.2. Mixed equivalent single layer models

The zigzag form of the displacement fields can be reproduced in Eq. (6) by employing the Murakami idea [12]. In the framework of the ESL description and according to Murakami a zigzag term can be introduced into Eq. (6) (see Fig. 2),

$$\boldsymbol{u}^k = \boldsymbol{u}_0 + (-1)^k \zeta_k \boldsymbol{u}_Z + z^r \boldsymbol{u}_r, \quad r = 1, 2, \ldots, N. \tag{9}$$

Subscript Z refers to the introduced zigzag term. With unified notations Eq. (10) becomes,

$$\begin{aligned} &\boldsymbol{u}^k = F_t \boldsymbol{u}_t + F_b \boldsymbol{u}_b + F_r \boldsymbol{u}_r = F_\tau \boldsymbol{u}_\tau, \quad \tau = t, b, r, \\ &\quad r = 1, 2, \ldots, N. \end{aligned} \tag{10}$$

Subscript t refers to the introduced zigzag term ($\boldsymbol{u}_t = \boldsymbol{u}_Z$, $F_t = (-1)^k \zeta_k$). The F_t functions assume the following explicit form. It should be noticed that F_t assumes the values ± 1 in correspondence to the bottom and the top interface of the k-layer (see Fig. 2).

The thickness expansion used for displacement variables in Eq. (10) is not suitable for the transverse stress cases. For instance, homogeneous top–bottom plate surface conditions cannot be imposed. Transverse stresses are therefore herein described by means of the layer-wise description [12,13,26–30]

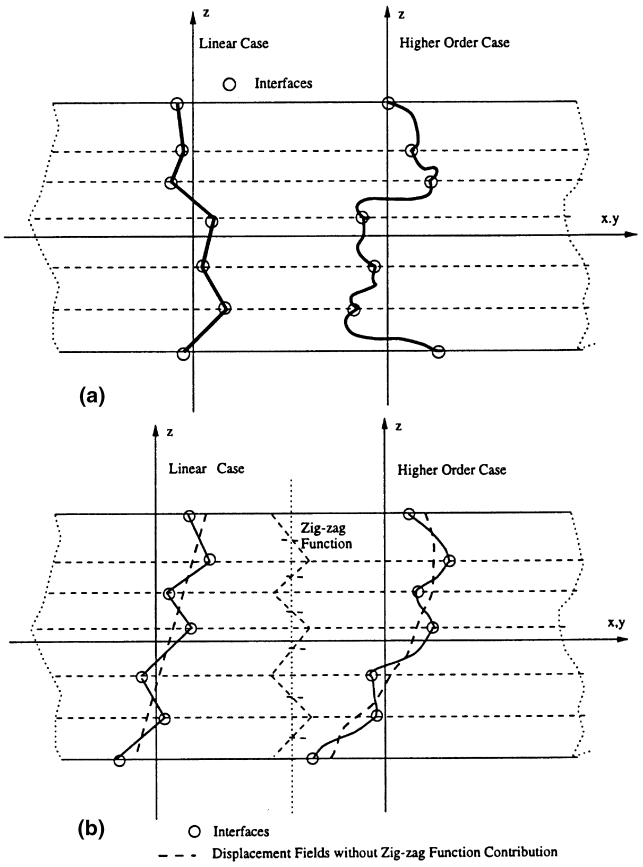

Fig. 2. Layer-wise (a) and equivalent single layer (b) fields assumed in the thickness plate directions. Classical ESLMs do not include zigzag function.

$$\begin{aligned} &\boldsymbol{\sigma}^k_{nM} = F_t \boldsymbol{\sigma}^k_{nt} + F_b \boldsymbol{\sigma}^k_{nb} + F_r \boldsymbol{\sigma}^k_{nr} = F_\tau \boldsymbol{\sigma}^k_{n\tau}, \\ &\quad \tau = t, b, r, \quad r = 2, 3, \ldots, N, \ k = 1, 2, \ldots, N_l. \end{aligned} \tag{11}$$

In contrast in Eq. (10), it is now intended that the subscripts t and b denote values related to the layer's top and bottom surfaces, respectively. They consist of the linear part of the expansion. The thickness functions $F_\tau(\zeta_k)$ have now been defined at the k-layer level,

$$\begin{aligned} &F_t = \frac{P_0 + P_1}{2}, \quad F_b = \frac{P_0 - P_1}{2}, \quad F_r = P_r - P_{r-2}, \\ &\quad r = 2, 3, \ldots, N, \end{aligned} \tag{12}$$

in which $P_j = P_j(\zeta_k)$ is the Legendre polynomial of the j-order defined in the ζ_k-domain: $-1 \leqslant \zeta_k \leqslant 1$. The parabolic, cubic and fourth-order stress fields equation (11) will be associated to linear, parabolic and cubic displacement field equation (10), respectively, in the numerical investigations. The related polynomials are

$$P_0 = 1, \quad P_1 = \zeta_k, \quad P_2 = (3\zeta_k^2 - 1)/2,$$
$$P_3 = \frac{5\zeta_k^3}{2} - \frac{3\zeta_k}{2}, \quad P_4 = \frac{35\zeta_k^4}{8} - \frac{15\zeta_k^2}{4} + \frac{3}{8}.$$

The chosen functions have the following properties:

$$\zeta_k = \begin{cases} 1: & F_t = 1; \quad F_b = 0; \quad F_r = 0, \\ -1: & F_t = 0; \quad F_b = 1; \quad F_r = 0. \end{cases} \tag{13}$$

The top and bottom values have been used as unknown variables. The interlaminar transverse shear and normal stress continuity can therefore be easily linked

$$\boldsymbol{\sigma}_{nt}^k = \boldsymbol{\sigma}_{nb}^{(k+1)}, \quad k = 1, \quad N_l - 1. \tag{14}$$

In those cases in which the top/bottom shell stress values are prescribed (zero or imposed values), the following additional equilibrium conditions must be accounted for:

$$\boldsymbol{\sigma}_{nb}^1 = \bar{\boldsymbol{\sigma}}_{nb}, \quad \boldsymbol{\sigma}_{nt}^{N_l} = \bar{\boldsymbol{\sigma}}_{nt}, \tag{15}$$

where the over-bar is the imposed values in correspondence to the plate boundary surfaces. Examples of linear and higher order fields have been plotted in Fig. 2. The stress variables could be eliminated by employing the *weak form of Hooke's law* proposed in [26]. The problem is therefore reduced to the displacement unknowns which are N_l independent. In such a sense these mixed theories have been considered of ESLM-type.

3.3. Layer-wise mixed and classical models

According to Carrera [26–30] two independent layer-wise fields are assumed for both displacement and stress variables as in Eq. (11),

$$\begin{aligned} &\boldsymbol{u}^k = F_t \boldsymbol{u}_t^k + F_b \boldsymbol{u}_b^k + F_r \boldsymbol{u}_r^k = F_\tau \boldsymbol{u}_\tau^k, \\ &\boldsymbol{\sigma}_{nM}^k = F_t \boldsymbol{\sigma}_{nt}^k + F_b \boldsymbol{\sigma}_{nb}^k + F_r \boldsymbol{\sigma}_{nr}^k = F_\tau \boldsymbol{\sigma}_{n\tau}^k, \\ &\quad \tau = t, b, r, \quad r = 2, 3, \ldots, N, \quad k = 1, 2, \ldots, N_l. \end{aligned} \tag{16}$$

In addition to Eq. (14) the compatibility of the displacement reads

$$\boldsymbol{u}_t^k = \boldsymbol{u}_b^{(k+1)}, \quad k = 1, \quad N_l - 1. \tag{17}$$

Classical layer-wise descriptions, formulated on the basis of principle of virtual displacements, do not assume any stress fields. Interlaminar continuity is therefore violated in such approaches.

4. Governing equations

In order to write all the models mentioned in the previous section it is convenient to refer to all the stress and displacement variables at the k-layer level, i.e. to use a layer-wise description. ESL cases are achieved by writing the governing equations at the multilayered plate level.

4.1. The k-layer

The displacement approach is formulated in terms of $\boldsymbol{u}^k$ by variationally imposing the equilibrium via the principle of virtual displacements. In the static case this establishes

$$\sum_{k=1}^{N_l} \int_{\Omega^k} \int_{A_k} \left(\delta \boldsymbol{\epsilon}_{pG}^{k\mathrm{T}} \boldsymbol{\sigma}_{p\mathrm{H}_d}^k + \delta \boldsymbol{\epsilon}_{nG}^{k\mathrm{T}} \boldsymbol{\sigma}_{n\mathrm{H}_d}^k \right) \mathrm{d}\Omega^k \, \mathrm{d}z = \delta L^{\mathrm{e}}, \tag{18}$$

where δ signifies virtual variations. The variation of the internal work has been split into in-plane and out-of-plane parts and involves the stress obtained from Hooke's law and the strain from the geometrical relations. δL^{e} is the virtual variation of the work done by the external layer-forces $\boldsymbol{p}^k$ ($\{p_x^k, p_y^k, p_z^k\}$).

In the mixed case, the equilibrium and compatibility are both formulated in terms of the $\boldsymbol{u}^k$ and $\boldsymbol{\sigma}_n^k$ unknowns via Reissner's mixed variational theorem [35,36]

$$\begin{aligned} \sum_{k=1}^{N_l} \int_{\Omega^k} \int_{A_k} \Big(& \delta \boldsymbol{\epsilon}_{pG}^{k\mathrm{T}} \boldsymbol{\sigma}_{p\mathrm{H}}^k + \delta \boldsymbol{\epsilon}_{nG}^{k\mathrm{T}} \boldsymbol{\sigma}_{nM}^k \\ & + \delta \boldsymbol{\sigma}_{nM}^{k\mathrm{T}} \left(\boldsymbol{\epsilon}_{nG}^k - \boldsymbol{\epsilon}_{n\mathrm{H}}^k \right) \Big) \mathrm{d}\Omega^k \, \mathrm{d}z = \delta L^{\mathrm{e}}. \end{aligned} \tag{19}$$

The LHS includes the variations of the internal work in the plate: the first two terms come from the displacement formulation, they lead to variationally consistent equilibrium conditions; the third 'mixed' term variationally enforces the compatibility of the transverse strains components.

Upon substitution of Eqs. (1)–(3) as well as of the requested assumed model Eqs. (6)–(16) and by integrating by parts, the two previous variational equations lead to governing differential equations. These equations were written in previous author's works in terms of stress and strain resultants; details on the treatment of the variational equations were also reported in these already mentioned works. For the sake of conciseness, the governing equations have herein been expressed in terms of the introduced stress and displacement variables.

The displacement formulation yields the following equilibrium conditions:

$$\delta \boldsymbol{u}_\tau^k : \boldsymbol{K}_d^{k\tau s} \boldsymbol{u}_s^k = \boldsymbol{p}_\tau^k \tag{20}$$

the related boundary conditions are

$$\boldsymbol{u}_\tau^k = \bar{\boldsymbol{u}}_\tau^k \quad \text{or} \quad \Pi_d^{k\tau s} \boldsymbol{u}_s^k = \Pi_d^{k\tau s} \bar{\boldsymbol{u}}_s^k, \tag{21}$$

while the mixed case leads to the following set of equilibrium and constitutive equations:

$$\begin{aligned} &\delta \boldsymbol{u}_\tau^k : \boldsymbol{K}_{uu}^{k\tau s} \boldsymbol{u}_s^k + \boldsymbol{K}_{u\sigma}^{k\tau s} \boldsymbol{\sigma}_{ns}^k = \boldsymbol{p}_\tau^k, \\ &\delta \boldsymbol{\sigma}_{n\tau}^k : \boldsymbol{K}_{\sigma u}^{k\tau s} \boldsymbol{u}_s^k + \boldsymbol{K}_{\sigma\sigma}^{k\tau s} \boldsymbol{\sigma}_{ns}^k = 0 \end{aligned} \tag{22}$$

and to the boundary conditions

$$\boldsymbol{u}_\tau^k = \bar{\boldsymbol{u}}_\tau^k \quad \text{or} \quad \Pi_u^{k\tau s} \boldsymbol{u}_s^k + \Pi_\sigma^{k\tau s} \boldsymbol{\sigma}_{ns}^k = \Pi_u^{k\tau s} \bar{\boldsymbol{u}}_s^k + \Pi_\sigma^{k\tau s} \bar{\boldsymbol{\sigma}}_{ns}^k. \tag{23}$$

Further subscript/superscript $s=t,b,r$ has been introduced in order to distinguish the terms related to the introduced variables from those related to their variations. In explicit form

$$\begin{aligned}
\boldsymbol{K}_d^{k\tau s} &= -\boldsymbol{D}_p^{\mathrm{T}}\left(\tilde{\boldsymbol{Z}}_{pp}^{k\tau s}\boldsymbol{D}_p + \tilde{\boldsymbol{Z}}_{pn}^{k\tau s}\boldsymbol{D}_{n\Omega} + \tilde{\boldsymbol{Z}}_{pn}^{k\tau s_z}\boldsymbol{D}_{n\Omega}\right)\\
&\quad - \boldsymbol{D}_{n\Omega}^{\mathrm{T}}\left(\tilde{\boldsymbol{Z}}_{np}^{k\tau s}\boldsymbol{D}_p + \tilde{\boldsymbol{Z}}_{nn}^{k\tau s}\boldsymbol{D}_{n\Omega} + \tilde{\boldsymbol{Z}}_{nn}^{k\tau s_z}\right)\\
&\quad + \tilde{\boldsymbol{Z}}_{np}^{k\tau_z s}\boldsymbol{D}_p + \tilde{\boldsymbol{Z}}_{nn}^{k\tau_z s}\boldsymbol{D}_{n\Omega} + \tilde{\boldsymbol{Z}}_{nn}^{k\tau_z s_z},\\
\boldsymbol{\Pi}_d^{k\tau s} &= \boldsymbol{I}_p^{\mathrm{T}}\left(\tilde{\boldsymbol{Z}}_{pp}^{k\tau s}\boldsymbol{D}_p + \tilde{\boldsymbol{Z}}_{pn}^{k\tau s}\boldsymbol{D}_{n\Omega} + \tilde{\boldsymbol{Z}}_{pn}^{k\tau s_z}\boldsymbol{D}_{n\Omega}\right)\\
&\quad + \boldsymbol{I}_{n\Omega}^{\mathrm{T}}\left(\tilde{\boldsymbol{Z}}_{np}^{k\tau s}\boldsymbol{D}_p + \tilde{\boldsymbol{Z}}_{nn}^{k\tau s}\boldsymbol{D}_{n\Omega} + \tilde{\boldsymbol{Z}}_{nn}^{k\tau s_z}\right),\\
\boldsymbol{K}_{uu}^{k\tau s} &= -\boldsymbol{D}_p^{\mathrm{T}}\boldsymbol{Z}_{pp}^{k\tau s}\boldsymbol{D}_p,\\
\boldsymbol{K}_{u\sigma}^{k\tau s} &= -\boldsymbol{D}_p^{\mathrm{T}}\boldsymbol{Z}_{pn}^{k\tau s} + E_{\tau_z s}\boldsymbol{I} - E_{\tau s}\boldsymbol{D}_{n\Omega}^{\mathrm{T}},\\
\boldsymbol{K}_{\sigma u}^{k\tau s} &= E_{\tau s}\boldsymbol{D}_{n\Omega} + E_{\tau s_z}\boldsymbol{I} - \boldsymbol{Z}_{np}^{k\tau s}\boldsymbol{D}_p,\\
\boldsymbol{K}_{\sigma\sigma}^{k\tau s} &= -\boldsymbol{Z}_{nn}^{k\tau s},\\
\boldsymbol{\Pi}_u^{k\tau s} &= \boldsymbol{I}_p^{\mathrm{T}}\boldsymbol{Z}_{pp}^{k\tau s}\boldsymbol{D}_p,\\
\boldsymbol{\Pi}_\sigma^{k\tau s} &= \boldsymbol{Z}_{pn}^{k\tau s} + E_{\tau s}\boldsymbol{I}_{n\Omega}^{\mathrm{T}},
\end{aligned} \tag{24}$$

where

$$\boldsymbol{D}_{n\Omega} = \begin{bmatrix} 0 & 0 & \partial_x \\ 0 & 0 & \partial_y \\ 0 & 0 & 0 \end{bmatrix}, \quad \boldsymbol{I} = \begin{bmatrix} 1 & 0 & 0 \\ 0 & 1 & 0 \\ 0 & 0 & 1 \end{bmatrix},$$

$$\boldsymbol{I}_p = \begin{bmatrix} 1 & 0 & 0 \\ 0 & 1 & 0 \\ 1 & 1 & 0 \end{bmatrix}, \quad \boldsymbol{I}_{n\Omega} = \begin{bmatrix} 0 & 0 & 1 \\ 0 & 0 & 1 \\ 0 & 0 & 0 \end{bmatrix}.$$

The integration in the thickness coordinate has been a priori carried out as usual in two-dimensional modelings: the following layer-stiffnesses and integrals have been introduced:

$$\begin{aligned}
&\left(\tilde{\boldsymbol{Z}}_{pp}^{k\tau s}, \tilde{\boldsymbol{Z}}_{pn}^{k\tau s}, \tilde{\boldsymbol{Z}}_{np}^{k\tau s}, \tilde{\boldsymbol{Z}}_{nn}^{k\tau s}, \boldsymbol{Z}_{pp}^{k\tau s}, \boldsymbol{Z}_{pn}^{k\tau s}, \boldsymbol{Z}_{np}^{k\tau s}, \boldsymbol{Z}_{nn}^{k\tau s}\right)\\
&\quad = \left(\tilde{\boldsymbol{C}}_{pp}^{k}, \tilde{\boldsymbol{C}}_{pn}^{k}, \tilde{\boldsymbol{C}}_{np}^{k}, \tilde{\boldsymbol{C}}_{nn}^{k}, \boldsymbol{C}_{pp}^{k}, \boldsymbol{C}_{pn}^{k}, \boldsymbol{C}_{np}^{k}, \boldsymbol{C}_{nn}^{k}\right)E_{\tau s},\\
&\left(\tilde{\boldsymbol{Z}}_{pn}^{k\tau s_z}, \tilde{\boldsymbol{Z}}_{np}^{k\tau_z s}, \tilde{\boldsymbol{Z}}_{nn}^{k\tau s_z}, \tilde{\boldsymbol{Z}}_{nn}^{k\tau_z s}, \tilde{\boldsymbol{Z}}_{nn}^{k\tau_z s_z}\right)\\
&\quad = \left(\tilde{\boldsymbol{C}}_{pn}^{k}E_{\tau s_z}, \tilde{\boldsymbol{C}}_{np}^{k}E_{\tau_z s}, \tilde{\boldsymbol{C}}_{nn}^{k}E_{\tau s_z}, \tilde{\boldsymbol{C}}_{nn}^{k}E_{\tau_z s}, \tilde{\boldsymbol{C}}_{nn}^{k}E_{\tau_z s_z}\right),\\
&\left(E_{\tau s}^{k}, E_{\tau_z s}, E_{\tau s_z}, E_{\tau_z s_z}^{k}\right)\\
&\quad = \int_{A_k}\left(F_\tau F_s, F_{\tau_z}F_s, F_\tau F_{s_z}, F_{\tau_z}F_{s_z}\right)\mathrm{d}z.
\end{aligned} \tag{25}$$

Explicit forms of the governing equations for each layer can be written by expanding the introduced subscripts and superscripts in the previous arrays as follows

$$k = 1,2,\ldots,N_l; \quad \tau = t,r,b, \quad s = t,r,b \quad (r = 2,\ldots,N).$$

4.2. The multilayered plate

In the previous sections, mixed and standard displacement formulations have been written for the N_l independent layers. Multilayered equations can be written according to the usual variational statements: stiffness and/or compliances related to the same variables are accumulated in this process. Interlaminar continuity conditions are imposed at this stage. Details on this procedure can be found in the already mentioned papers. Multilayered arrays are introduced. The equilibrium and boundary conditions for the displacement formulation take on the following form:

$$\begin{aligned}
&\boldsymbol{K}_d\boldsymbol{u} = \boldsymbol{p},\\
&\boldsymbol{u} = \bar{\boldsymbol{u}} \quad \text{or} \quad \boldsymbol{\Pi}_d\boldsymbol{u} = \boldsymbol{\Pi}_d\bar{\boldsymbol{u}},
\end{aligned} \tag{26}$$

while for the mixed case, one has

$$\begin{aligned}
&\boldsymbol{K}_{uu}\boldsymbol{u} + \boldsymbol{K}_{u\sigma}\boldsymbol{\sigma}_n = \boldsymbol{p} + \boldsymbol{p}_u^{1N_l},\\
&\boldsymbol{K}_{\sigma u}\boldsymbol{u} + \boldsymbol{K}_{\sigma\sigma}\boldsymbol{\sigma}_n = \boldsymbol{p}_\sigma^{1N_l}
\end{aligned} \tag{27}$$

with boundary conditions

$$\boldsymbol{u} = \bar{\boldsymbol{u}} \ \text{ or } \ \boldsymbol{\Pi}_u\boldsymbol{u} + \boldsymbol{\Pi}_\sigma\boldsymbol{\sigma}_n = \boldsymbol{\Pi}_u\bar{\boldsymbol{u}} + \boldsymbol{\Pi}_\sigma\bar{\boldsymbol{\sigma}}_n. \tag{28}$$

$\boldsymbol{p}_u^{1N_l}$ and $\boldsymbol{p}_\sigma^{1N_l}$ are the arrays obtained from the transverse stress values imposed at the top/bottom of the plate.

4.3. Closed form solutions for orthotropic plates

The boundary value problem governed by Eqs. (26)–(28) in the most general case of geometry, boundary conditions and lay-outs, could be solved by implementing only approximated solution procedures. The particular case in which the material has the properties $\tilde{C}_{16} = \tilde{C}_{26} = \tilde{C}_{36} = \tilde{C}_{45} = 0$, has here been considered. Navier-type closed form solutions can be found by assuming the following harmonic forms for the applied loadings and unknown variables:

$$\begin{aligned}
\left(u_{x_\tau}^k, \sigma_{xz_\tau}^k, p_{x_\tau}^k\right) &= \sum_{m,n}\left(U_x^k, S_{xz_\tau}^k, P_{x_\tau}^k\right)\cos\frac{m\pi x}{a}\sin\frac{n\pi y}{b},\\
\left(u_{y_\tau}^k, \sigma_{yz_\tau}^k, P_{y_\tau}^k\right) &= \sum_{m,n}\left(U_y^k, S_{yz_\tau}^k, P_{y_\tau}^k\right)\sin\frac{m\pi x}{a}\cos\frac{n\pi y}{b},\\
\left(u_{z_\tau}^k, \sigma_{zz_\tau}^k, p_{z_\tau}^k\right) &= \sum_{m,n}\left(U_z^k, S_{zz_\tau}^k, P_{z_\tau}^k\right)\sin\frac{m\pi x}{a}\sin\frac{n\pi y}{b},
\end{aligned} \tag{29}$$

a and b are the plate lengths in the x and y directions, respectively, while m and n are the correspondent wave numbers. Capital letters in the RHS are correspondent maximum amplitudes. On substitution of Eq. (29), the governing equations assume the form of a linear system of algebraic equations. This procedure has been coded for the different case theories and results are discussed in Section 5.

5. Results and discussion

Simply supported plates bent by a transverse bisinusoidal distribution of normal pressure $p_{z_t}^{N_l}$ applied to

the top surface of the whole plate have been considered. Two loading cases $m=1$, $n=0$ (cylindrical bending) and $m=n=1$ have been examined. The theories discussed in Section 6 have been all implemented. A vast numerical investigation has been conducted directly to compare a priori and a posteriori evaluations of transverse normal and shear stresses. Selected results are presented in what follows. Acronyms have been introduced to denote the different analysis in tables and diagrams. Three characters have been used to build up these acronyms. The first character can be L or E which states Layer-wise or Equivalent single layer analysis. The second one can be M or D which states Mixed or classical analysis on the basis of Displacement formulation. The third character can assume the numbers 1, 2, 3 or 4 which state the order N of the stress and displacement fields. For instance, LM3 means Layer-wise Mixed analysis with cubic stress and displacement field in each layer. A suffix has been added to the acronyms wherever transverse stress results are quoted: -A, -H and -I denote stresses obtained by the assumed model, by Hooke's law and by integration of the 3D-indefinite equilibrium equations, respectively. Assessment and comparison to exact solution and to other available two-dimensional analyses have been provided in Tables 1 and 2. Thin and thick as well as square and rectangular plate geometries have been analyzed. Cross-ply, symmetrically ($N_l=3$) and unsymmetrically ($N_l=4$) laminated plates are considered. Transverse displacements of thick plates are considered in Table 1. The mixed models by Murakami [12] and Toledano and Murakami [13] correspond (exception made of the fact that σ_{zz} effect was neglected in [12]) to the present EM1 and EM3 cases, respectively. A good agreement between present and referenced mixed models has been found. Comparison to other refined models [10,15], (suffix l and c denote linear and cubic expansion, respectively) demonstrates the superiority of mixed approaches. The following further comments can be made. Layer-wise analysis leads to excellent agreement with respect to exact solution. Such agreement barely depends on N_l. Mixed models show better performance than classical ones. These improvements are much more significant as far as ESLM analysis is concerned. The worst results of LM1 analysis must be addressed to the fact that the homogeneous conditions for the transverse stresses cannot been imposed for a linear stress field in the k-layer. Singularity of the matrix $\boldsymbol{K}_{\sigma\sigma}$ has been therefore avoided but the accuracy of the analysis decreases. EM1 case does not suffer from this drawback. In fact, a parabolic stress field is associated to a linear zigzag displacement field in this case. Parabolic terms play a significant role in ESLM analysis of unsymmet-

Table 1
Maximum transverse displacement $\bar{U}_z = U_z \times 100 E_T h^3/(P_{z_t}^{N_l} a^4)$ $(z=0)$ of thick plates in cylindrical bending [a]

	$a/h=4$		$a/h=6$	
	$N_l=3$	$N_l=4$	$N_l=3$	$N_l=4$
Exact	2.887	4.181	1.635	2.556
[13]	2.881	4.105	1.634	2.519
[15]-c	–	4.083	–	2.501
[12]	2.907	3.316	1.636	2.107
[15]-l	–	3.316	–	2.107
[10]	2.687	3.587	1.514	2.242
Present LWM analysis				
LM4	2.887	4.181	1.635	2.556
LM3	2.887	4.181	1.635	2.556
LM2	2.891	4.181	1.635	2.556
LM1	2.791	4.163	1.599	2.542
LD4	2.887	4.180	1.635	2.556
LD3	2.887	4.180	1.635	2.556
LD2	2.864	4.166	1.630	2.553
LD1	2.783	4.059	1.583	2.496
Present ESLM analysis				
EM3	2.881	4.102	1.634	2.514
EM2	2.831	3.478	1.602	2.195
EM1	2.904	3.300	1.634	2.095
ED4	2.687	3.830	1.514	2.362
ED3	2.685	3.596	1.514	2.238
ED2	2.074	2.984	1.209	1.952
ED1	2.091	2.925	1.211	1.917

[a] Comparison of present analyses to exact solutions by Pagano [3] and to other available two-dimensional theories. Mechanical data of the lamina are $E_L/E_T = 25$, $G_{LT}/E_T = G_{Lz}/E_T = 0.50$, $G_{TT}/E_T = 0.2$, $\nu_{LT} = \nu_{Lz} = \nu_{TT} = 0.25$.

Table 2
Influence of thickness ratio on both $\bar{U}_z = U_z \times 100 E_T h^3/(p_{z_t}^{N_l} a^4)$ and $\bar{S}_{xz} = S_{xz}/(P_{z_t}^{N_l} a/h)$. Rectangular ($b = 3a$) three-layered plates. Exact solution by Pagano [3]. Mechanical data are those of Table 1

a/h	$\bar{U}_z$			$\bar{S}_{xz}$			
		4	10	20	4	10	20
Exact	2.820	0.919	0.610	–	0.387	0.420	0.434
[19]	2.729	0.918	0.609	I	0.378	0.441	0.451
[18]-l	2.717	0.881	0.599	I	0.366	0.419	–
[18]-c	2.757	0.919	0.610	I	0.329	0.420	–
[11]	2.80	0.920	–	I	0.317	0.415	–
LWM mixed analysis							
LM4	2.821	0.919	0.610	A	0.386	0.420	0.434
				H	0.386	0.420	0.434
				I	0.386	0.420	0.434
LM3	2.822	0.919	0.610	A	0.387	0.420	0.434
				H	0.473	0.426	0.439
				I	0.387	0.420	0.434
LM2	2.825	0.919	0.610	A	0.394	0.422	0.435
				H	0.396	0.421	0.434
				I	0.391	0.420	0.434
LM1	2.730	0.910	0.608	A	0.347	0.417	0.433
				H	0.365	0.458	0.479
				I	0.396	0.418	0.434
LWM classical analysis							
LD4	2.821	0.919	0.610	H	0.386	0.420	0.434
				I	0.387	0.421	0.434
LD3	2.821	0.919	0.610	H	0.390	0.420	0.434
				I	0.386	0.420	0.434
LD2	2.798	0.918	0.610	H	0.459	0.419	0.434
				I	0.389	0.420	0.434
LD1	2.721	0.899	0.604	H	0.356	0.420	0.434
				I	0.395	0.421	0.435
ESLM mixed analysis							
EM3	2.815	0.919	0.610	A	0.422	0.427	0.441
				H	0.442	0.426	0.440
				I	0.388	0.420	0.434
EM2	2.767	0.906	0.606	A	0.365	0.429	0.444
				H	0.355	.424	0.438
				I	0.393	0.421	0.435
EM1	2.839	0.915	0.606	A	0.399	0.459	0.476
				H	0.368	0.435	0.450
				I	0.388	0.420	0.525
ESLM classical analysis							
ED4	2.625	0.867	0.595	H	0.612	0.307	0.312
				I	0.378	0.427	0.596
ED3	2.627	0.867	0.595	H	0.613	0.307	0.312
				I	0.378	0.427	0.436
ED2	2.035	0.752	0.566	H	0.399	0.158	0.158
				I	0.437	0.439	0.439
ED1	2.051	0.750	0.563	H	0.414	0.158	0.158
				I	0.437	0.439	0.439

rically laminated plates. N-order decreasing EM and ED results are very much affected by N_l. Thick and thin plates are considered in Table 2. σ_{zz} is neglected in the referenced two-dimensional solutions [11,18,19]. As far as transverse displacement is concerned comments made for Table 1 are confirmed. The three manners of computing transverse shear stresses are compared for all the implemented theories (quoted stresses are located in $z = 0$ unless $a/h = 4$ case, for which the maximum stress values have been detected). Hooke's law results, related to mixed formulation equations (2) could not lead to transverse stresses, which have been assumed in this case. In this paper the classical form of Hooke's law Eq. (1), has been forced even though mixed analyses is referred to. It is expected that such an inconsistency would conduce to poor accuracy of related transverse stresses.

The good performance of layer-wise modelings found for U_z should be extended to the transverse stress results of Table 2. For the fourth-order cases ($N=4$) -A, -H, and -I type values merge. As expected, LM-H results are poorer than LD-H ones. This fact does not happen for the ESLM analysis: the improvements introduced by mixed description with respect to classical ones are much more significant than of layer-wise cases (for instance LD type analysis describes zigzag effects, ED one does not). Assumed a priori results LM2-A, LM3-A and LM4-A show excellent agreement with respect to 3D solutions. a/h increasing LM-A and LM-I results merge. These results confirm [28,30] the effectiveness of modelings based on Reissner's mixed variational theorem. LM4-H, LD4-H and LD3-H results are in excellent agreement to the exact solution. That is Hooke's law can be seen as a valuable tool to compute transverse stress supposing that an adequate LWM is implemented. Unfortunately, such accuracy is in any case restricted to LWMs and rapidly decreases by N-decreasing. In fact, ESLMs results show poorer description for all the implemented order N. It should be observed that -I type analysis has led to the better description in all the considered modelings. The discrepancy among -I, -A and -H types results very much increases for the ESLM results with respect to LW results.

Through-the-thickness distributions of transverse stresses have been plotted in Figs. 3–6. The three manners to calculate transverse stresses are compared. Results related to different N-order and to thick and thin plates have been drawn. Fig. 3 refers to layer-wise evaluations. The fourth-order case shows that -A, -H and -I type curves coalesce. For purpose of comparison LM4-I curve has been included in the diagrams related to lower order cases. Major differences can be seen for the third-order expansion case. It is confirmed that

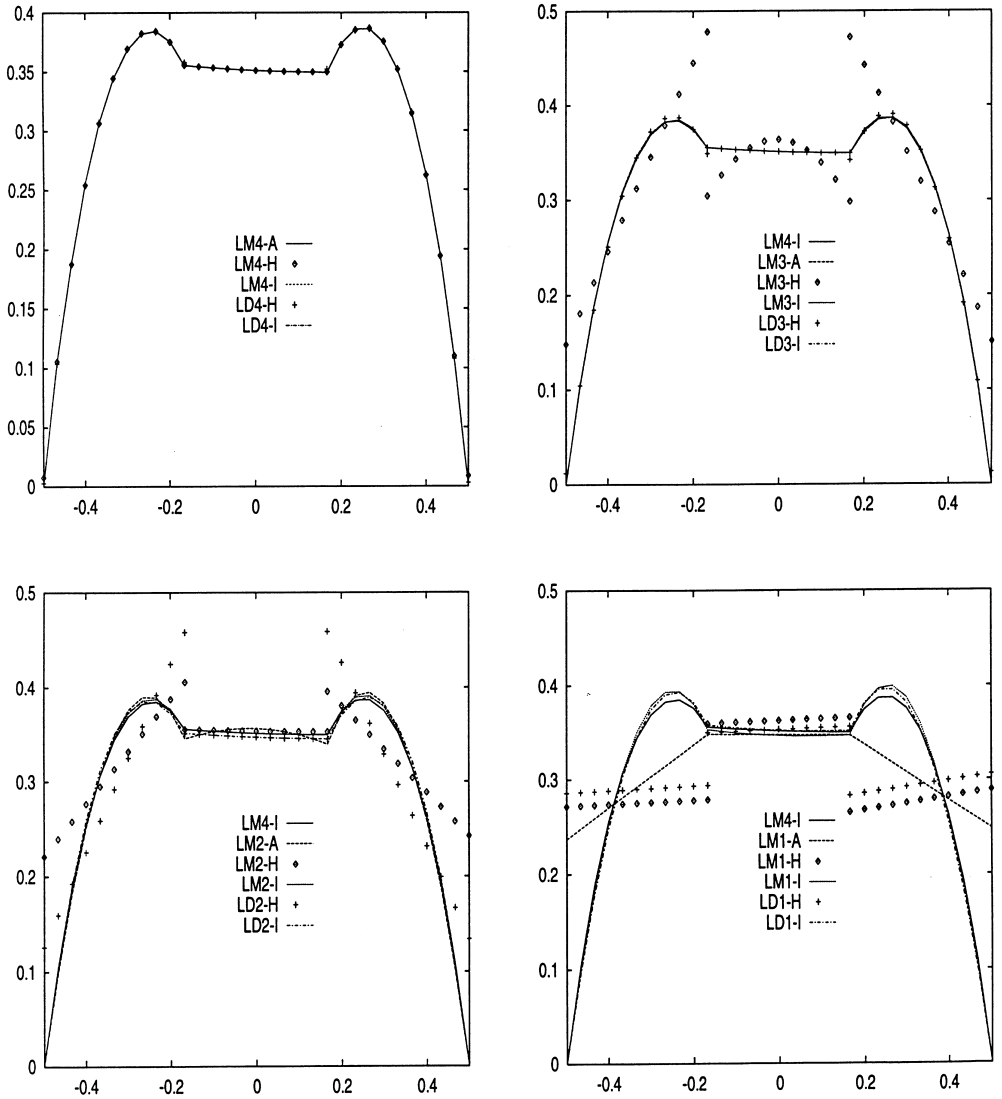

Fig. 3. $S_{xz}/(p_{z_t}^{N_t}a/h)$ vs z/h. A priori vs. a posteriori evaluation for mixed and classical layer-wise models. Data are those of Table 2 ($a/h=4$).

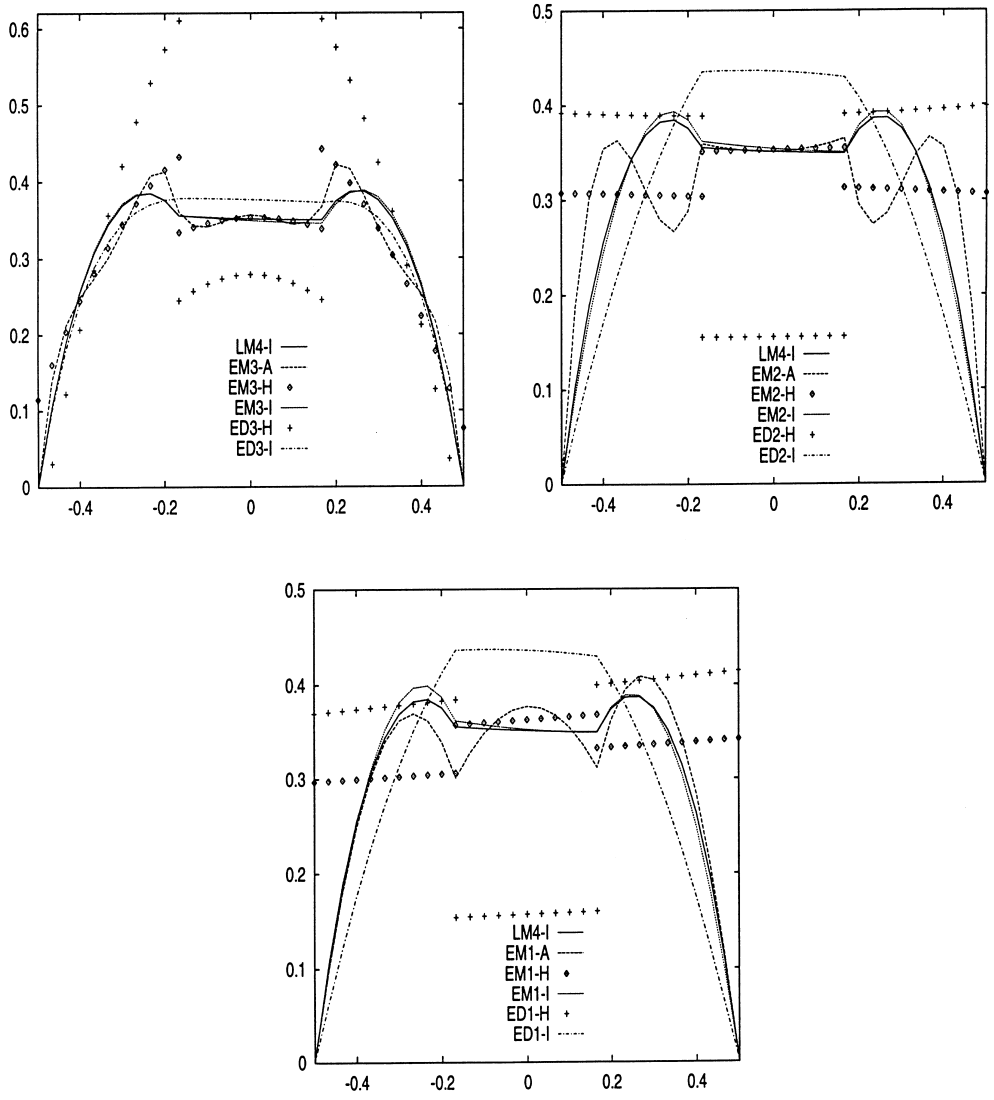

Fig. 4. $S_{xz}/(p_{z_t}^{N_l}a/h)$ vs. z/h. A priori vs. a posteriori for mixed and classical equivalent single layer models. Data are those of Table 2 ($a/h=4$).

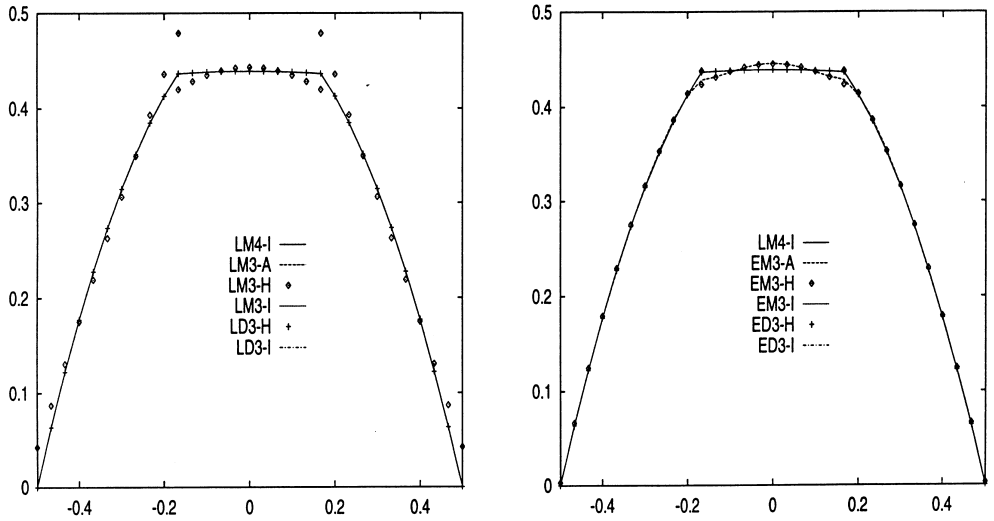

Fig. 5. $S_{xz}/(p_{z_t}^{N_l}a/h)$ vs. z/h. A priori vs. a posteriori for mixed and classical LW and ESL models (third-order case). Data are those of Table 2 ($a/h=100$).

LM3-H result leads to poor results: LM3-H analysis violates interlaminar equilibria. The same happens for LM2-H, LM1-H as well as for LD2-H and LD1-H analyses. N-order decreasing, the difference among different evaluations increases. LM3-I and LM2-I leads to the best description. LM-A analysis has in any case acceptable accuracy exception made for the LM1-A case as discussed in Table 2. ESLM results are presented in Fig. 4. Mixed analysis are much more accurate than classical ones (EM-I and EM-H are more accurate than ED-I and ED-H, respectively, for all the considered N-order). To be noticed is that differences among the presented analyses are in this case much higher then LWM results of Fig. 3. EM3-I, EM2-I and EM1-I lead to results which are the closest to those of LM4-I. It is noticed that depending on z/h, EM-A calculations can be more accurate than ED-I ones. -H type analyses lead to the poorest accuracy: interlaminar equilibria is violated in all the investigated cases. A thin plate has been considered in Fig. 4 where comparison has been restricted to the third order cases. LM4-I has been plotted for comparison purpose. As well known, the discrepancy between mixed and classical analysis (both LW and ESLM cases) disappears in thin plate geometry. On the one hand the differences among the different manners to evaluate stresses have been preserved for thick plates. In particular LM3-H is still poor. Transverse normal stress results of thin and thick plate for third order theories are compared in Fig. 6. LM4-I, LM3-A and LD3-3I results merge. LM3-H and LD3-H show interlaminar discontinuous transverse normal stress. Also in this case, the use of inconsistent Hooke's law leads to LM3-H results which are poorer than LD3-H ones. It is of certain interest to note that LM3-I curves do not fulfill the

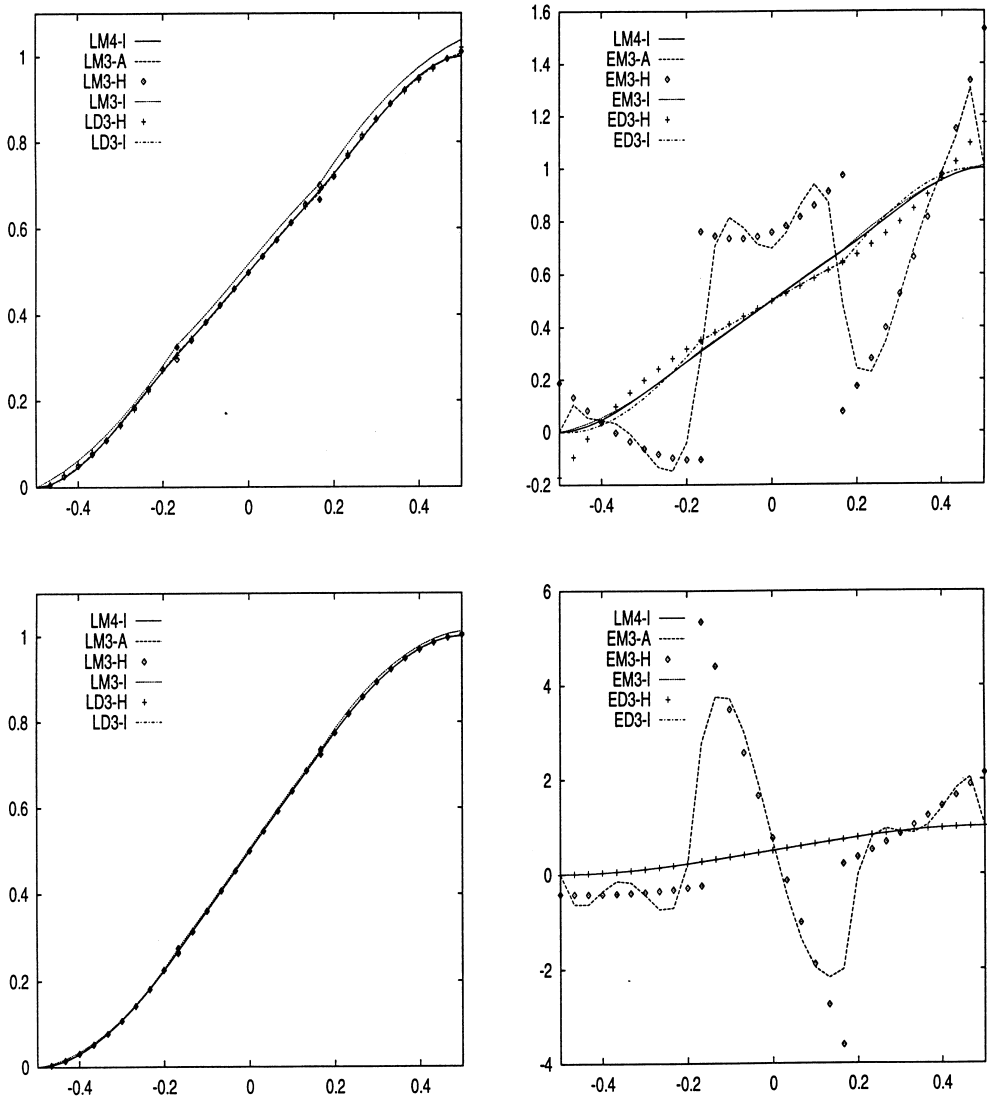

Fig. 6. $S_{zz}/p_{z_t}^{N_t}$ vs. z/h. A priori vs. a posteriori for mixed and classical LW and ESL models (third-order case). Upper and lower couples of diagrams are related to thick ($a/h=4$) and thin ($a/h=100$) plates, respectively. Further data are those of Table 2.

boundary condition on the top plate: the unit value is barely violated. This result must be addressed to the fact the I-types evaluations have been done a posteriori. There is no theoretical reason which excludes such a result: different results could be obtained by starting the integration of the 3D equilibrium equations from the top surface with respect to those obtained by starting from the bottom surface of the plate. This fact would

Table 3
A priori vs. a posteriori evaluation of transverse shear stresses $\sigma_{yz}/P_{z_l}^{N_l}$ (at $z=0$) [a]

a/h	E_L/E_T	3D	LM3			LD3		EM3			ED3	
			A	H	I	H	I	A	H	I	H	I
10	3	2.380	2.380	2.395	2.380	2.380	2.380	2.373	2.520	2.378	2.813	2.378
	30	2.344	2.344	2.383	2.344	2.344	2.344	2.383	2.517	2.343	2.825	2.342
5	3	1.185	1.185	1.193	1.185	1.185	1.185	1.182	1.255	1.180	1.400	1.181
	30	1.141	1.141	1.166	1.141	1.141	1.141	1.167	1.235	1.136	1.383	1.135

[a] Comparison of present analyses to 3D solution by Noor and Burton [6]. Square plates, cross-ply, skew-symmetric laminated with $N_l=10$. Mechanical data of the lamina are: $G_{LT}/E_T = G_{Lz}/E_T = 0.50$, $G_{TT}/E_T = 0.35$, $\nu_{LT} = \nu_{Lz} = 0.30$, $\nu_{TT} = 0.49$. Hooke's law values refer to the 90° oriented lamina.

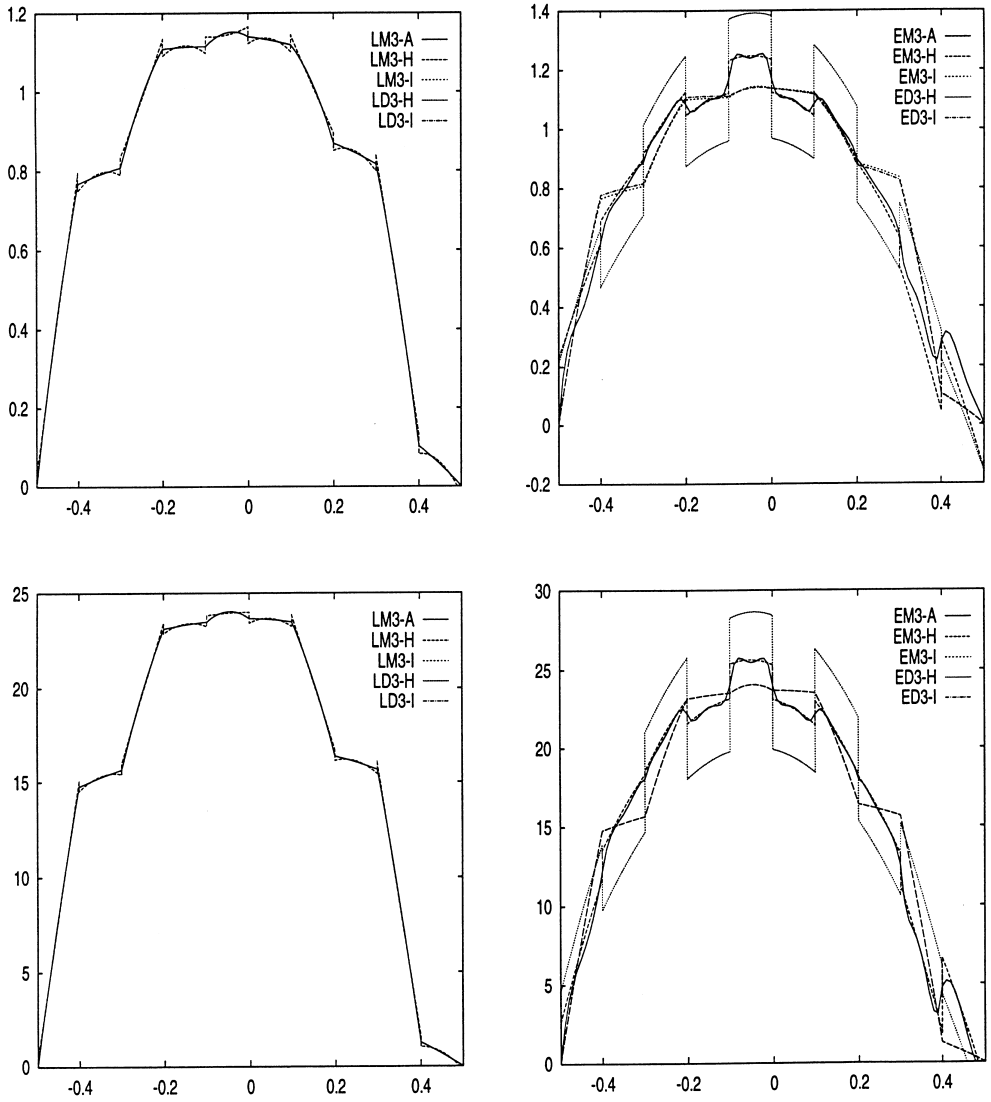

Fig. 7. $S_{yz}/p_{z_l}^{N_l}$ vs. z/h. A priori vs. a posteriori for mixed and classical LW and ESL models (third-order case). Upper and lower couples of diagrams are related to thick ($a/h=5$) and thin ($a/h=100$) plates, respectively. Further data are those of Table 3.

suggest assessing -I types results with other analyses before taking them as good ones. The differences between ESLM and LW analyses are in this case higher than those registered for shear stress cases. In particular EM3-A results are very inaccurate, so that, one can confirm [27,28] the fundamental limitation of any equivalent single layer theories to accurately describe σ_{zz} and related effects. Layer-wise description is required for this purpose. The differences among -A, -H and -I type evaluations of σ_{zz} are scarcely affected by the plate thickness ratio.

In order to show the influences of in-plane out-of-plane strain couplings as well as of increasing number of layers N_l a test problem previously investigated by Noor and Burton [6] has been re-considered in Table 3 and Figs. 7 and 8. A thin-layered skew symmetric, square, cross-ply laminated plate has been analyzed for the third-order cases. Two values of thickness ratio and of orthotropic ratio are considered. a/h increasing as well as E_l/E_t decreasing ESLM and LW modelings merge. The deviation among -A, -H and -I type evaluation is scarcely influenced by these two ratios. It is confirmed that LW predictions are not influenced by laminate lay-outs. The conclusions reached for the symmetrically layered case are confirmed by Table 3 and Figs. 7 and 8 with the following amendments. Hooke's law evaluation of transverse shear and normal stresses related to classical theories ED3-H as well as EM3-A results of unsymmetrically laminated plates are poorer than those obtained for the symmetrically laminated plates (this conclusion was tested by many other examples not quoted herein). This fact confirms that -A, -H and -I type evaluations related to ESLM analysis are very much influenced by laminate lay-outs.

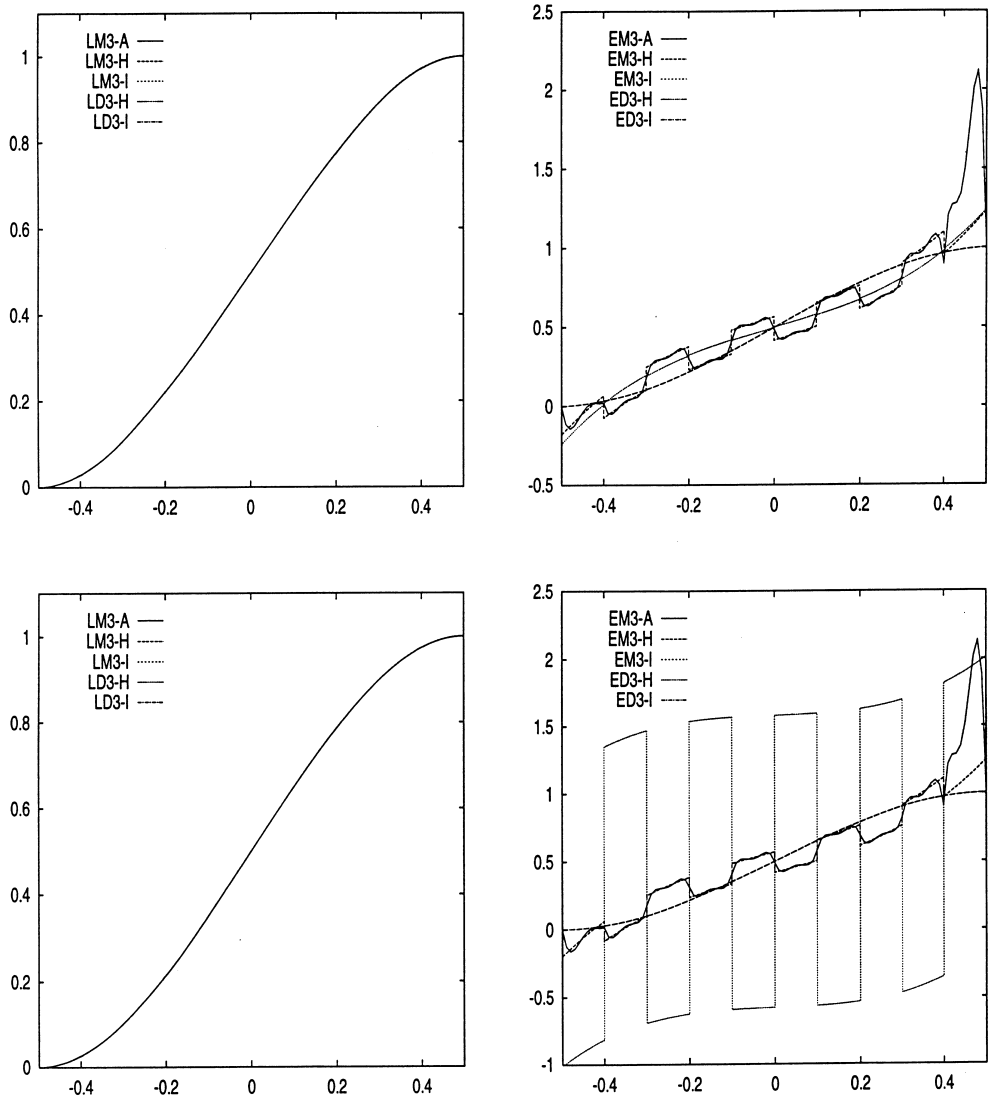

Fig. 8. $S_{zz}/p_{z_t}^{N_l}$ vs. z/h. A priori vs. a posteriori for mixed and classical LW and ESL models (third-order case). Upper and lower couples of diagrams are related to thick ($a/h=5$) and thin ($a/h=100$) plates, respectively. Further data are those of Table 3.

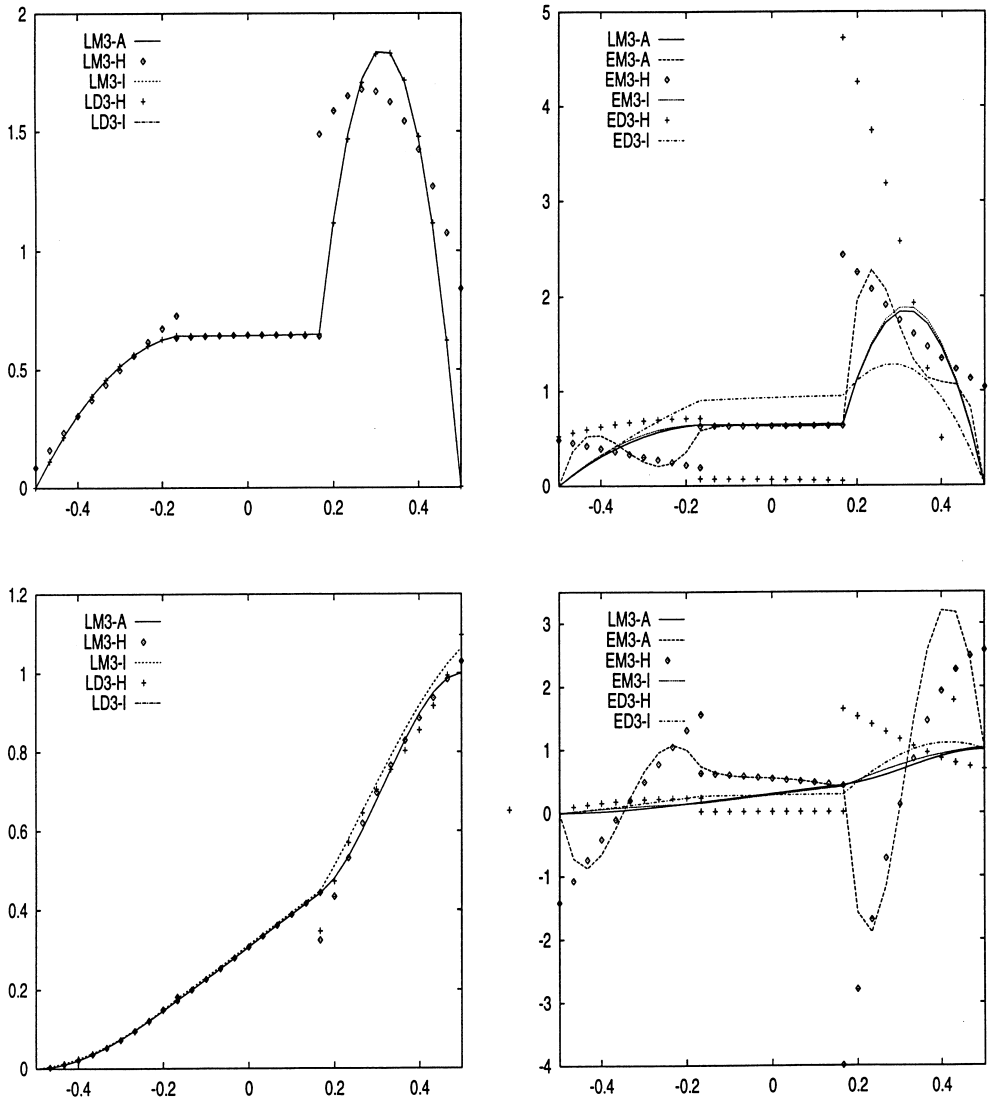

Fig. 9. $S_{xz}/p_{z_l}^{N_l}$ (upper couple of diagrams) vs. z/h and $S_{zz}/p_{z_l}^{N_l}$ (lower couple of diagrams) vs. z/h. A priori vs. a posteriori for mixed and classical LW and ESL models (third-order case). Three-layered square plate made of isotropic layers ($a/h = 5$).

The influence of a non-constant distribution of Young modulus E_z in the thickness direction has been considered in Fig. 9. A three-layered thick plate constituted by isotropic ($\nu = 0.3$) layers has been investigated. The plate is an unsymmetrically laminated plates with $E^1/E^2 = 10$; $E^3/E^2 = 100$, where E^k (k = 1, 2, 3) are the Young moduli of the three layers. The superiority of the ESLM mixed analysis over the related displacement ones is more evident than in the previously investigated plates, e.g. EM3-A is much more accurate than ED3-I.

6. Conclusions

This paper has compared three manners to evaluate transverse shear and normal stresses in multilayered plates. A priori stresses have been obtained by employing mixed models formulated on the basis of Reissner's mixed variational theorem. A posteriori calculations have been performed by using Hooke's law and by integration of the three-dimensional indefinite equilibrium equations. Classical formulations based on displacement assumptions have been also considered. Both LW and ESLM have been implemented. Linear up to fourth order stress and/or displacement fields in the layer-plate thickness direction have been considered. The conducted investigation restricted to bending of simply supported plate made of orthotropic layers have mainly led to the following conclusions:

1. Layer-wise analysis furnishes quasi-three-dimensional description of transverse stresses of laminate thick plates, while the accuracy of ESLM analyses is very much subordinate to laminate lay-outs and to the mechanical properties of the lamina. The superiority of

mixed analyses has been confirmed with respect to classical ones, especially as far as ESLM is concerned.
2. The accuracy of the different modelings is very much subordinate to the order N of the used stress and displacement expansion. Very accurate layer-wise results have been obtained for $N \geqslant 2$.
3. The discrepancy among the three manners of evaluating transverse shear stresses is scarcely dependent on plate thickness ratio.
4. Hooke's law furnishes very accurate evaluation of transverse shear and normal stresses for layer-wise theories. Third and fourth-order expansions are requested for classical and mixed cases, respectively. ESLM accuracy is very poor even though higher N-order are considered. Furthermore, such accuracy is very much subordinate to the multilayered plate lay-outs.
5. Transverse stresses evaluated by integration of the 3D indefinite equilibrium equations have led, in general, to the best description. As inconvenient, in some cases such a posteriori procedure could fail to fulfill stress boundary conditions at the top/bottom plate surface.

Acknowledgements

The author is deeply indebted to two eminent Scientists who recently passed away. The late Professor Eric Reissner for his encouragement to work on the subject of this paper and the late Professor Placido Cicala for the essential suggestions and criticisms given during the review process of the paper [26].

References

[1] Washizu K. Variational method in elasticity and plasticity. Oxford: Pergamon, 1968.
[2] Reddy JN. Mechanics of Laminated Composite Plates. Theory and Analysis Boca Raton: CRC Press, 1997.
[3] Pagano NJ. Exact solutions for composite laminates in cylindrical bending. J Composite Mater 1969;3:398–411.
[4] Srinivas S, Rao AK. Bending, vibration and buckling of simply supported thick orthotropic rectangular plates and laminates. Int J Solids and Structures 1970;30:495–507.
[5] Pagano NJ, Hatfield SJ. Elastic behavior of multilayered bidirectional composites. Amer Inst Aeronautics Astronautics J 1972:931–33.
[6] Noor AK, Burton WS. Stress and free vibration analyses of multilayered composite plates. Composite Struct 1989;11:183–204.
[7] Lekhnitskii SG. Strength calculation of composite beams. Vestnik inzhen. i tekhnikov 1935;9.
[8] Ambartsumian SA. On general theory of anisotropic shells. PMM 1968;22(2):226–37.
[9] Whitney JM. The effects of transverse shear deformation on the bending of laminated plates. J Composite Mater 1969;3:534–47.
[10] Lo KH, Christensen RM, Wu EM. A higher-order theory of plate deformation Part 2: laminated plates. J Appl Mech 1977;44:669–76.
[11] Ren JG. A new theory for laminated plates. Composite Sci and Technol 1986;26:225–39.
[12] Murakami H. Laminated composite plate theory with improved in-plane response. J Appl Mech 1986;53:661–6.
[13] Toledano A, Murakami H. A higher-order laminated plate theory with improved in-plane responses. Int J Solids and Structures 1987;23:111–31.
[14] Bhashar B, Varadan TK. Refinement of higher-order laminated plate theories. Amer Inst Aeronautics Astronautics J 1989;27:1830–1.
[15] Cho M, Parmerter RR. Efficient higher order composite plate theory for general lamination configurations. Amer Inst Aeronautics Astronautics J 1993;31:1299–305.
[16] Hodges DH, Lee BW, Atilgan AR. Application of the variational-asymptotic method to laminated composite plates. Amer Inst Aeronautics Astronautics J 1993;31:1674–983.
[17] Satyrin VG, Hodges DH. On asymptotically correct linear laminated plate theory. Int J Solids and Structures 1996;33:3649–71.
[18] Di Sciuva M. A general quadrilater multilayered plate element with continuous interlaminar stresses. Composite Struct 1993;47:91–105.
[19] Idlbi A, Karama M, Touratier M. Comparison of various laminated plate theories. Composite Struct 1997;37:173–84.
[20] Hsu T, Wang JT. A theory of laminated cylindrical shells consisting of layers of orthotropic laminae. Amer Inst Aeronautics Astronautics J 1970;8:2141–6.
[21] Srinivas S. A refined analysis of composite laminates. J Sound and Vib 1973;30:450–95.
[22] Toledano A, Murakami H. A composite plate theory for arbitrary laminated configurations. J Appl Mech 1987a;54:181–9.
[23] Barbero EJ, Reddy JN, Teply JL. General two-dimensional theory of laminated cylindrical shells. Amer Inst Aeronautics Astronautics J 1990;28:544–53.
[24] Robbins DH. Jr, Reddy JN. Modeling of thick composites using a layer-wise theory. Int J Numer Methods Engrg. 1993;36:655–77.
[25] Gaudenzi P, Barboni R, Mannini A. A finite element evaluation of single-layer and multi-layer theories for the analysis of laminated plates. Composite Struct 1995;30:427–40.
[26] Carrera E. A class of two dimensional theories for multilayered plates analysis. Atti Accademia delle Scienze di Torino, Mem Sci Fis 1995;19-20:49–87.
[27] Carrera E. C_z^0-requirements: models for the two-dimensional analysis of multilayered structures. Composite Struct 1997;37:373–84.
[28] Carrera E. Evaluation of layer-wise mixed theories for laminated plates analysis. Amer Inst Aeronautics Astronautics J 1998;36:830–9.
[29] Carrera E. Mixed layer-wise theories for multilayered plates analysis. Composite Struct 1998;43:57–70.
[30] Carrera E. Layer-wise mixed models for accurate vibration analysis of multilayered plates. J Appl Mech 1998;65:820–9.
[31] Sun CT, Whitney JM. On the theories for the dynamic response of laminated plates. Amer Inst Aeronautics Astronautics J 1973;11:372–98.
[32] Librescu L, Reddy JN. A critical review and generalization of transverse shear deformable anisotropic plates. In: Elishakoff I, Irretier H editors. Euromech colloquium 219, Kassel, September 1986, 'refined dynamical theories of beams, plates and shells and their applications, Springer, Berlin, 1987, pp. 32–43.
[33] Kapania RK, Raciti S. Recent advances in analysis of laminated beams and plates. Amer Inst Aeronautics Astronautics J 1989;27:923–46.
[34] Noor AK, Burton WS. Assessment of shear deformation theories for multilayered composite plates. Appl Mech Rev 1989;41:1–18.
[35] Reissner E. On a certain mixed variational theory and a proposed applications. Int J Numer Methods Engrg 1984;20:1366–8.

[36] Reissner E. On a mixed variational theorem and on a shear deformable plate theory. Int J Numer Methods Engrg 1986; 23:193–8.
[37] Reissner E. Reflections on the theory of elastic plates. Appl Mech Rev 1985;38:1433–64.
[38] Carrera E. Single-layer vs multi-layers plate modelings on the basis of Reissner's mixed theorem. J Appl Mech (in press).
[39] Carrera E. Transverse normal stress effects in multilayered plates. Amer Inst Aeronautics Astronautics J (in press).